Xiangang Wan, Masanori Kohno and Xiao Hu Computational Materials Science Center, National Institute for Materials Science, Tsukuba 305-0047, Japan

Abstract

By means of the LSDA+U method and the Green function method, we investigate the electronic and magnetic properties of the new material of $Sr_8CaRe_3Cu_4O_{24}$. Our LSDA+U calculation shows that this system is an insulator with a net magnetic moment of 1.01 $\mu_B/f.u.$, which is in good agreement with the experiment. Magnetic moments are mainly located at Cu atoms, and the magnetic moments of neighboring Cu sites align anti-parallel. It is the non-magnetic Re atoms that induce an orbital order of d electrons of Cu atoms, which is responsible for the strong exchange interaction and the high magnetic transition temperature. Based on the LSDA+U results, we introduce an effective model for the spin degrees of freedom, and investigate the finite-temperature properties by the Green function method. The obtained results are consistent with the experimental results, indicating that the spin-alternating Heisenberg model is suitable for this compound.

75.30.Et, 75.10.Jm, 75.10.-b, 71.70.Gm

Perovskite transition-metal oxides have been investigated intensively [1]. The discoveries of high- T_c superconductivity [2] and colossal magnetoresistance (CMR) [3] in this family of materials pose significant challenge to theoretical understanding of the strongly correlated electron systems.

In certain parameter regimes, strong Coulomb repulsions make electrons localized and the materials behave as Mott insulators. In this phase, low-energy excitations are dominated by the superexchange interaction [4], and the collective excitations of spin degrees of freedom govern the physics. Undoped high- T_c superconductors (HTC) are such typical examples. Their properties are well described by a spin-1/2 antiferromagnetic (AFM) Heisenberg model on a square lattice. It is widely believed that properties of the undoped systems are closely related to the origin of high- T_c superconductivity [5].

It is also well known that the charge distribution in perovskite transition-metal oxides is influenced strongly by the crystal field, i.e. the degeneracy of the 3d electrons is lifted by lattice distortions of the perovskite structure in various ways. Therefore, the spin, charge and orbital degrees of freedom are intervened with each other, which make the physics of the perovskite transition-metal oxides very rich. These features are shared by materials in which CMR are observed [6].

As will be revealed in this Letter, the recently synthesized material $Sr_8CaRe_3Cu_4O_{24}$, which forms the cubic perovskite structure as shown in Fig. 1(a), is another member of this family of materials [7]. The new material is similar to the undoped HTC in the following aspects: (1) perovskite structure, (2) magnetic insulator, (3) Cu surrounded by O. However, it is different in the points that this material is three-dimensional and has nonzero magnetization in the ground state $M \simeq 0.95\mu_B$ per formula unit (f.u.) Also, this compound is peculiar since ferromagnetic (FM) cuprates are very rare, and has an unusually high magnetic transition temperature $T_c \simeq 440$ K. Curie temperatures T_c of known FM cuprates are usually quite low. For example, the T_c of La₄BaCu₂O₁₀, K₂CuF₄ and SeCuO₃ are 5, 6.5, and 26 K, respectively [8]. Therefore, it is interesting to see why a strong FM state is realized in this material. Although the response of the compound to carrier doping is also very interesting, we will concentrate here on the undoped material. It is shown that both the electron-electron correlation and the coupling between orbital and spin degrees of freedom are important for this compound, which results in an spin-alternative Heisenberg Hamiltonian.

We calculate the electronic and magnetic structures of $Sr_8CaRe_3Cu_4O_{24}$ by using the WIEN2K package [9], which is an implementation of the density-functional APW+lo method [10]. The MT sphere radii of 2.0, 2.0, 2.0, 1.9 and 1.5 a.u. are chosen for the Ca, Cu, Sr, Re, and O atoms, respectively, with $RK_{max}=7.0$, which results in about 5,200 LAPWs and local orbitals per cell. We use 700 k points in the Brillouin zone. As for the exchange-correlation potential, we adopt the standard generalized gradient approximation (GGA) [11]. Our GGA calculation predicts this material as a metal inconsistent with the experiment, which indicates that the electron-electron interactions are important for this compound. Thus, we use the LSDA+U method [12] to take them into account, and adopt U=10 eV and J=1.20 eV for the d orbital of Cu [13].

In order to investigate the magnetic structures and interactions of $Sr_8CaRe_3Cu_4O_{24}$, we calculate both AFM and FM configurations for Cu1 and Cu2 moments. The results are shown in Table I. Magnetic moments are mainly located at Cu1 and Cu2 sites in both

configurations with the magnitude almost independent of the configuration. The magnetic moments at Ca, Sr, O1 and O3 are smaller than 0.001 $\mu_{\rm B}$. Thus, they are negligible compared to the moments at Cu. O2 carries a small but nonvanishing moment due to large hybridization with Cu1 and Cu2. Our numerical results show that the AFM configuration is the ground state with net magnetic moment $M=1.01 \ \mu_{\rm B}/{\rm f.u.}$ This is quantitatively consistent with the experimental one. Also, the ground state is an insulator with the energy gap of 1.68 eV consistently with the experimental result [7]. It should be noted that the magnetic moment at Re atom is very small (less than 0.004 $\mu_{\rm B}$) in both configurations. This feature is contrasted with the ordered double perovskite A₂Fe MO_6 , where due to the hybridization with d orbitals of Fe, the non-magnetic ion M possesses a large magnetic moment and plays a significant role in the magnetic properties [14,15]. We also performed calculations for U=8and 12 eV to cover a wide range of generally accepted values of correlations. Numerical results show that the magnetic moments are not sensitive to U. With decreasing U, the energy difference between AFM and FM (ΔE) increases slightly. For example, the calculated ΔE for U=8 eV is higher than that of U=10 eV by about 20%.

Figure 2(a) shows the calculated charge density plotted in (010) plane of Fig. 1(a). The charge density along the Re-O3 bonds is larger than that along Cu2-O3, indicating a stronger bond for Re-O3 than that for Cu2-O3. Therefore, the O3 atom is attracted toward Re. This induces a Jahn-Teller distortion in the oxygen octahedron centered at Cu2 consisting of four O3 and two O2 atoms with the bond length of Cu2-O2 smaller than that of Cu2-O3. Consequently, the e_g orbital of Cu2 splits into $d_{3z^2-r^2}$ and $d_{x^2-y^2}$. The former which points to O2 has a higher energy than the latter. Thus as shown in Fig. 3(b), the partially occupied orbital in Cu2 is the minority spin (spin-up) $d_{3z^2-r^2}$, and the charge density distribution of Cu2 is anisotropic as shown in Fig. 2(a). In contrast, three crystallographic directions of cu1 are completely equivalent, and the oxygen octahedron centered at Cu1 site is free of any distortion. Therefore, the e_g orbital of Cu1 is still fully degenerate, and all d orbitals except for the minority spin (spin-down) in the e_g orbital are fully occupied as shown in Fig. 3(a). In addition, the 2p states of O2 distribute mainly in the energy range from -7.0 to 0.0 eV, and are almost full-filling.

The spin density shown in Fig. 2(b) clearly indicates that the magnetic moments of the Cu1 and Cu2 are carried mostly by e_g and $d_{3z^2-r^2}$ orbitals, respectively. In Fig. 4, we schematically show the partially occupied d orbitals of Cu1 and Cu2 and the almost fully occupied p_z orbital of O2 for the material. It is interesting to observe that an orbital ordering appears at Cu sites. Namely, the minority spin $d_{3z^2-r^2}$ orbital of Cu2 and the e_g orbital of Cu1 are pointing to the O2 as shown in Fig. 4. Both of them are less than half-filling. Meanwhile, the fully occupied p_z orbital of O2 points to the neighboring Cu1 and Cu2 sites. Therefore, the spin-up and -down p_z orbitals of O2 strongly overlap with the spin-up $d_{3z^2-r^2}$ of Cu2 and the spin-down e_g orbital of Cu1, respectively, to form a rather strong $pd\sigma$ hybridization. This results in a strong exchange interaction between the magnetic moments at Cu1 and Cu2 and a high transition temperature.

In order to further clarify the effects of Re, we perform a calculation for an artificial structure, where the Jahn-Teller distortion in oxygen octahedron centered at Cu2 is removed. We find that the orbital ordering still survives, and the results are very similar to that of the real structure. We then change Re to Technetium, which is the element at the same column in the periodic table. Our calculation shows that the partially occupied orbital of Cu2

changes from $d_{3z^2-r^2}$ to $d_{x^2-y^2}$. Consequently, the spin and the orbital are almost decoupled, and the spin interaction becomes much weaker. As a result, the energy difference between AFM and FM configurations is reduced greatly. Therefore, the Re atoms play an important role for the orbital ordering to cause the unusually high T_c , although their magnetic moments are very small.

Since the magnetic moments are almost localized at Cu sites, the effective model for the spin degrees of freedom of this material is expected to be a Heisenberg model, where neighboring localized spins at Cu sites interact antiferromagnetically. Although, the simple ionic model (Cu²⁺-O²⁻ or Cu³⁺-O²⁻) is not exact due to the large hybridization between Cu and O, we still take spins at Cu sites as a good quantum number similar to the case of the undoped HTC. We consider the following two cases: (1)S₁=1, S₂=1/2 and (2) S₁=S₂=1/2, where S_i denotes the spin length at Cui site. The magnetization in the unit cell for the AFM state and that of the FM state are obtained as (1) $M_{\rm AFM}=1/2$, $M_{\rm FM}=5/2$ and (2) $M_{\rm AFM}=1$, $M_{\rm FM}=2$. The LSDA+U result is $M_{\rm AFM}=1.01 \ \mu_{\rm B} \simeq 0.5$, $M_{\rm FM}=5.01 \ \mu_{\rm B} \simeq 2.5$ as shown in Table I. Hence, case (1) is reasonable. Thus, the effective Hamiltonian becomes the following:

$$H = J_{\text{eff}} \sum_{i} S_i \cdot \sum_{p} s_{i+\frac{p}{2}},\tag{1}$$

where J_{eff} is the effective exchange interaction, *i* runs over Cu1 sites, and *p* denotes the unit vectors of the unit cell in the lattice shown in Fig. 1(b) $(p=\pm \hat{x},\pm \hat{y},\pm \hat{z})$. Here, S_i and $s_{i+\frac{p}{2}}$ denote the spin operator of S=1 at Cu1-site(*i*) and that of S=1/2 at Cu2-site($i+\frac{p}{2}$), respectively.

Since this model is on a bipartite lattice and belongs to the family in which the Marshall-Lieb-Mattis theorem holds [16], the ground state of this model is proven to have spin $S=1/2(=1/2\times 3-1)$ in any size of systems. This results in spontaneous magnetization M=1 $\mu_{\rm B}$ in the bulk limit, and well explains the experimental result ($M \simeq 0.95 \mu_{\rm B}$ [7]).

Since the difference of the magnitude of magnetic moments at Cu sites between FM and AFM states is small as shown in Table I, the energy difference between FM and AFM $\Delta E=0.036$ Ry=5,679 K can be assigned to the exchange interaction. By diagonalizing the Hamiltonian (1) in the unit cell, we evaluate the energy difference between FM and AFM configuration as $8J_{\text{eff}}$. Hence, we estimate $J_{\text{eff}}=\Delta E/8=710$ K. Using the above effective Hamiltonian, we investigate magnetic properties of Sr₈CaRe₃Cu₄O₂₄. In order to take quantum fluctuations into account, we apply the Green function method [17]. In this method, we construct sixteen Green functions of Cu1-spins and Cu2-spins. We use Tyablikov's decoupling [18] to obtain closed coupled equations for Green functions. Following Callen's scheme [19], we obtain $\langle s^z \rangle$ and $\langle S^z \rangle$. Thus, we solve these coupled equations numerically to obtain $\langle s^z \rangle$ and $\langle S^z \rangle$ at finite temperatures.

The result of the Green function method for the spontaneous magnetization is shown in Fig. 5. In the low-temperature limit, spontaneous magnetization M obtained by the Green function method is about $1\mu_{\rm B}$, which is consistent with the exact result M=1 $\mu_{\rm B}$ and the experimental result $M \simeq 0.95 \ \mu_{\rm B}$. Magnetic transition temperature $T_{\rm c}$ is calculated as $T_{\rm c} = 448$ K by the Green function method, which is close to the experimental result $T_{\rm c} \simeq 440$ K. Thus, the magnetic properties known so far in Sr₈CaRe₃Cu₄O₂₄ are explained by the spin-alternating Heisenberg model defined in eq.(1). Here, we summarize the mechanism of ferrimagnetism and the high magnetic transition temperature T_c for Sr₈CaRe₃Cu₄O₂₄. The mechanism of the AFM coupling is the superexchange [4]. The large exchange constant J_{eff} is due to the large overlap between Cu and O2 orbitals, and to the localization of Cu-spins by strong correlations. This situation is similar to the case of the undoped HTC. In contrast to the undoped HTC, the number of sublattice sites is different. This causes ferrimagnetism. Imbalance of the spin length between Cu1 and Cu2 sites would also be a reason for stabilization of the ferrimagnetic state.

In summary, using the LSDA+U method and the Green function method, we have investigated the electronic and magnetic properties of $Sr_8CaRe_3Cu_4O_{24}$. Our results show that magnetic moments are almost located at Cu sites, and the moments of Cu1 and Cu2 align anti-parallel due to the superexchange interaction [4]. The ground state is a ferrimagnetic insulator with a net magnetic moment of $1.01 \ \mu_B/f.u.$, which is in good agreement with the experimental results. We find that the non-magnetic transition metal Re plays an important role in determining the magnetic properties of this material. Namely, Re induces orbital orderings of the *d* orbitals in Cu. This results in the strong exchange coupling between the magnetic moments of Cu and the unusually high T_c . Based on the LSDA+U results, we have introduced an effective model for the spin degree of freedom, and investigated the magnetic properties by the Green function method. The ground-state magnetization of this model is shown to be exactly 1 μ_B , which is consist with the experimental result. The obtained T_c is also consistent with the experimental one. Therefore, the spin-alternating Heisenberg model is suitable for describing the magnetic properties of this compound.

We acknowledge Dr. E. Takayama-Muromachi for bringing our attentions to this material and for valuable discussions. Dr. M. Arai and Dr. M. Katakiri are appreciated for technical helps. This work was partially supported by Japan Society for the Promotion of Science (Grant-in-Aid for Scientific Research (C) No. 15540355).

REFERENCES

- See, for example, M. Imada, A. Fujimor, and Y. Tokura, Rev. Mod. Phys. 70, 1039 (1998).
- [2] J. G. Bednorz and K. A. Muller, Zeit. Phys. B 64, 189 (1986).
- [3] S. Jin *et al.*, Science **264**, 413 (1994); P. Schiffer *et al.*, Phys. Rev. Lett. **75**, 3336 (1995).
- [4] H.A. Kramers, Physica 1, 182 (1934); P.W.Anderson, Phys. Rev. 115, 2 (1959).
- [5] F.C. Zhang and T.M. Rice, Phys.Rev.B **37**, 3759 (1988).
- [6] C.N.R. Cao *et al.*, J. Phys.: Condens. Matter **12**, R83 (2000); M.B. Salamon and M. Jaime, Rev. Mod. Phys. **73**, 583 (2001).
- [7] E. Takayama-Muromachi et al., J. Solid State Chem. **175**, 366 (2003).
- [8] F. Mizuno *et al.*, Nature (London) **345**, 788 (1990); I. Yamada, J. Phys. Soc. Jpn. **33**, 979 (1972); K. Kohn *et al.*, J. Solid State Chem. **18**, 27 (1976).
- [9] P. Blaha et al., WIEN2K, An Augmented Plane Wave + Local Orbitals Program for Calculating Crystal Properties (Karlheinz Schwarz, Tech. Universität Wien, Austria, 2001). ISBN 3-9501031-1-2.
- [10] E. Sjöstedt, L. Nordström, and D.J. Singh, Solid State Commun. **114**, 15 (2000); G.K.H. Madsen *et al*, Phys. Rev. B **64**, 195134 (2001).
- [11] J.P. Perdew, K. Burke and M. Ernzerhof, Phys. Rev. Lett. 77, 3865 (1996).
- [12] V.I. Anisimov, J. Zaanen and O.K. Andersen, Phys. Rev. B 44, 943 (1991); V.I. Anisimov *et al.*, Phys. Rev. B 48, 16929 (1993); M.T. Czyzyk, and G.A. Sawatzky, Phys. Rev. B 49, 14211 (1994).
- [13] V.I. Anisimov *et al.*, Phys. Rev. B **66**, 100502 (2002).
- [14] D.D. Sarma *et al.*, Phys. Rev. Lett. **85**, 2549 (2000).
- [15] Z. Fang, K. Terakura and J. Kanamori, Phys. Rev. B 63, 180407 (2001); J. Kanamori and K. Terakura, J. Phys. Soc. Jpn. 70, 1433 (2001).
- [16] W. Marshall, Proc. Roy. Soc. A 232, 48 (1955); E.H. Lieb and D. Mattis, J. Math. Phys. 3, 749 (1962).
- [17] N.N. Bogolyubov and S.V. Tyablikov, Dokl. Acad. Nauk. SSSR **126**,53 (1959)
 [Sov.Phys.Dokl. **4**, 604 (1959)].
- [18] S.V. Tyablikov, Ukr. Mat. Zh. **11**, 287 (1959).
- [19] H.B. Callen, Phys. Rev **130**, 890 (1963).

TABLES

TABLE I. Calculated total energy, E_{tot} relative to the energy of AFM configuration in units of Ry, the total magnetic moments per unit cell μ_{tot} , the magnetic moment at Cu1, Cu2 and O2 in units of μ_B .

	E_{tot}	μ_{tot}	Cu1	Cu2	O2
FM	0.036	5.01	1.15	0.84	0.14
AFM	0.0	-1.01	1.09	-0.81	0.07

FIGURES

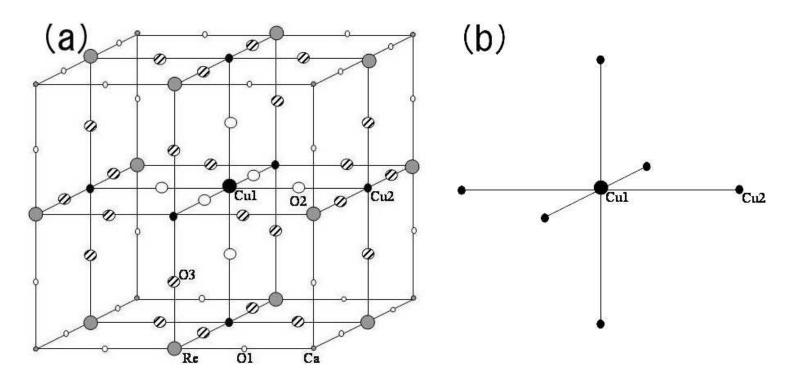
FIG. 1. Crystal structure of $Sr_8CaRe_3Cu_4O_{24}$. (a) Unit cell. (b) Unit cell of the effective model.

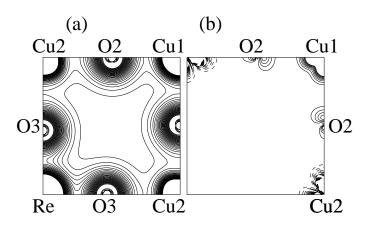
FIG. 2. Contours for charge density in the (010) plane with interval 0.03 e/bohr^3 . (a) Total charge density. (b) Spin density (spin-up charge density minus spin-down charge density). The dotted lines are negative contours.

FIG. 3. Projected density of state with Fermi energy at zero. (a) For minority spin (spin-down) d orbital of Cu1. (b) For minority spin (spin-up) d orbital of Cu2.

FIG. 4. Schematic picture for the spin and orbital orders of $Sr_8CaRe_3Cu_4O_{24}$ deduced from the LSDA+U calculation. The gray symbols denote partially occupied *d* orbital, and the dark ones denote full-occupied *p* orbital. The arrows denote the directions of magnetic moments on Cu sites.

FIG. 5. Temperature dependence of the spontaneous magnetization. Solid curve denotes the Green function result. Squares and the dotted line are experimental results in Ref.[7].





arXiv:cond-mat/0405684 v1 30 May 2004

